

Improved Potentiometric and Optic Sensitivity of Polyaniline Film to Dissolved Oxygen by Incorporating Iron-Porphyrin

Meng Li,^[a] Isabel M. Ornelas,^[b] Wei Liu,^[a] Yu Niu,^[a] Jorge P. Correia,^[b] Ana S. Viana,^[b] and Gang Jin^{*[a]}

Abstract: Polyaniline (PAN) films can be used in an electrochemical and optical combination system to amplify the optical signal for dissolved oxygen (DO) detection. To further improve the sensitivity of PAN film to DO, an oxygen-sensitive molecule, Fe(III) meso-tetra (4-sulfonatophenyl) porphyrin (FeTSPP) is incorporated into PAN during the film generation. Results show that, after incorporating FeTSPP into the PAN matrix, both optical and

potentiometric responses to DO are improved. The optimal optical signal is obtained under the application of $-2.5 \mu\text{A}$ to the modified electrode. Under this applied current, both optical and potentiometric signals show linear relations with the DO concentration within the range of $0.00\text{--}4.63 \text{ mg L}^{-1}$, and the sensitivities for optical and potentiometric signals are $4.18 \text{ grayscale units mg}^{-1}\text{L}$ and $13.39 \text{ mV mg}^{-1}\text{L}$, respectively.

Keywords: Dissolved oxygen • Electrochemical and optical combination sensor • Fe(III) meso-tetra (4-sulfonatophenyl) porphyrin (FeTSPP) • Polyaniline • Total internal reflection imaging ellipsometry (TIRIE)

1 Introduction

Detecting dissolved oxygen (DO) concentration is of great importance in chemical, biochemical, environmental, industrial and medical applications [1]. The conventional method for DO detection is iodine titration [2]. However, this method is not of practical application, as it involves several chemical reactions, being quite time-consuming (and chemicals-consuming as well), and cannot be used for *in situ* real-time measurements [2]. Consequently, great effort has been devoted to the development of alternative DO sensors [3–8] that are accurate and with fast response. Most of the reported approaches are built on the Clark electrode and its modified forms [3–5]. Despite popular application of the Clark electrode, it has an especially significant drawback in that its signal is unstable due to the consumption of the silver counter electrode [9]. As a result, Clark-type oxygen sensors need frequent and elaborate precalibration, especially for long-term measurements [9,10]. To overcome the problem of signal drift, an optical and electrochemical integrated methodology has been proposed based on total internal reflection imaging ellipsometry (TIRIE) [11]. In this combination system (EC-TIRIE), a gold film coated on a glass slide is used as both the working electrode and the optical sensing surface, producing simultaneous optical and electrochemical signals that can be easily monitored. Since the two signals can corroborate each other, this combination system provides a reliable method to validate the DO readings. The initial results obtained by this combination system confirm the feasibility of the methodology. However using only the gold film the optical signal change is very small. From oxygen-free to oxygen-containing solution, the optical signal change is less than 2 grayscale

units [11]. To amplify the optical signal, an electronically conducting polymer, polyaniline (PAN), is used to cover the gold film surface due to its specific optical and electrochemical properties. PAN suffers structural modifications depending on its oxidation state and the pH of the medium, which are accompanied by color changes [12–14]. In acidic solution, PAN can suffer two redox transitions, being oxidized from its fully reduced, or leucoemeraldine state (benzenoid structure; pale yellow) to its partially oxidized and conductive state, emeraldine (radical cation intermediate form; combination of quinoid and benzenoid structures; green), and further to its fully oxidized, pernigraniline state (quinoid structure; blue) [13,14]. When exposed to oxygen, PAN is spontaneously oxidized from the leucoemeraldine to the emeraldine state, evidenced by a change in the polymer color [14–18].

The results obtained with the combination system using a PAN-modified gold film (Au-PAN) confirm that PAN has the ability to amplify the optical signal of the combination system for DO detection [11]. Nevertheless, under optimal conditions the optical signal achieved by Au-PAN

[a] M. Li,[#] W. Liu, Y. Niu, G. Jin
NML, Institute of Mechanics, Chinese Academy of Sciences,
15 Bei-si-huan West Road, Beijing 100190, China
*e-mail: gajin@imech.ac.cn

[b] I. M. Ornelas,[#] J. P. Correia, A. S. Viana
CQB, Faculdade de Ciências da Universidade de Lisboa,
Edifício C8, Campo Grande, 1749-016 Lisboa, Portugal

[#] These authors contribute equally to this article

 Supporting Information for this article is available on the WWW under <http://dx.doi.org/10.1002/elan.201400678>.

is about 10 units in the TIRIE grayscale, which is still very limited.

In order to improve the sensitivity of PAN to DO monitoring and further amplify the TIRIE signal, an Fe(III) coordination compound, highly responsive to oxygen, is incorporated into the PAN matrix in this work. The insertion of compounds with a high affinity for molecular oxygen into the polymeric matrix can increase the sensitivity of the modified electrode towards DO detection. Some oxygen reduction catalysts, such as phthalocyanine metal complexes [19] or noble metal catalysts [20,21] can be immobilized in conducting polymer matrices to improve the films' sensitivity to oxygen [19]. Transition metal complexes, including Co and Fe-containing metalloporphyrins, have been extensively explored as catalysts for electrochemical reduction of molecular oxygen [22–25]. They have been used in hybrid structures mixed with polyaniline derivatives [26] or as composite catalysts along with other transition metal oxides [27].

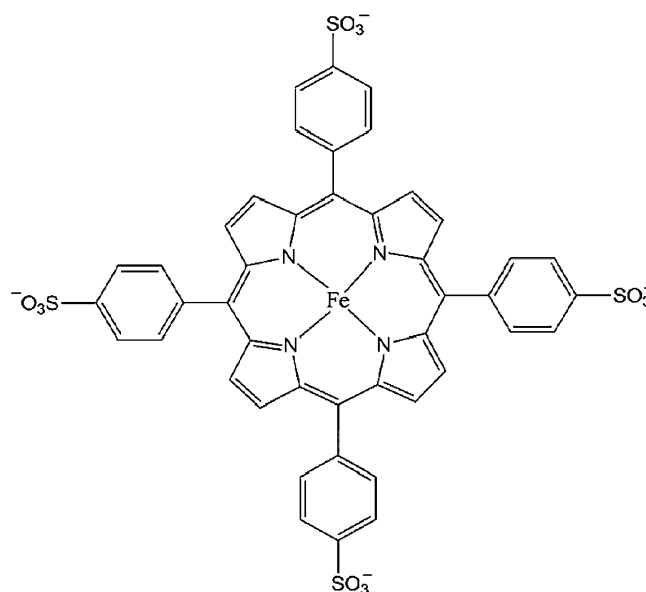
In this paper, Fe(III) meso-tetra (4-sulfonatophenyl) porphyrin (FeTSPP) is incorporated into PAN films to improve the sensitivity of PAN to DO and further amplify the optical signal. This compound was chosen for two main reasons: 1) Iron porphyrins catalyze the oxygen reduction reaction by being themselves oxidized in a reversible process [28]; 2) due to its anionic groups and relative (to aniline) big size, FeTSPP should be efficiently entrapped into the polymeric matrix of PAN by codeposition during its electropolymerization. It is expected that iron porphyrin will enhance the modified electrode's response to oxygen by acting as a mediator, being oxidized by oxygen and regenerated by the PAN matrix, resulting in a color change of the film.

Initially, the FeTSPP is characterized electrochemically by cyclic voltammetry (CV) in O₂-containing solution to confirm its electrocatalytic activity towards the oxygen reduction reaction (ORR). After that, modified electrodes of polyaniline containing the iron-porphyrin (PAN-FeTSPP) are prepared by doping-entrapment in the polymeric matrix during its electrochemical generation. The electrochemical conditions of the synthesis of the PAN-FeTSPP films are optimized to obtain the amplified optical signal for DO detection. The surfaces of PAN and PAN-FeTSPP films were characterized by atomic force microscopy (AFM) imaging in order to assess the effect of the introduction of the porphyrin into the polymeric matrix on film morphology. Finally, the dynamic responses of the EC-TIRIE (electrochemistry-total internal reflection imaging ellipsometry) sensor to different concentrations of DO are studied and working curves for this combination system are obtained.

2 Experimental

2.1 Chemicals

Na₂HPO₄ (≥99.0%), KH₂PO₄ (≥99.5%), H₂SO₄ (95–98%) (Sinopharm Chemical Reagent Co., Ltd) and ani-

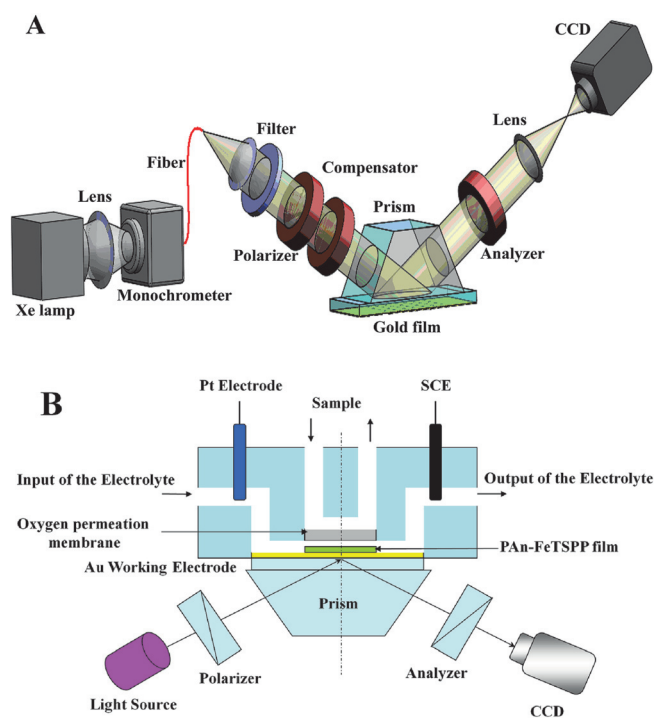


Scheme 1. Structure of Fe(III) meso-tetra (4-sulfonatophenyl) porphyrin (FeTSPP).

line (99.7%) (J&K Scientific Ltd.) were used without any further purification. The tetra-sodium Fe(III) meso-tetra (4-sulfonatophenyl) porphyrin (FeTSPP, Scheme 1) was purchased from Frontier Scientific(U.S.A.). Sodium sulfite (BioXtra, ≥98%) was obtained from Sigma-Aldrich. Ultrapure water was obtained from MILLI-Q purification system (18.2 MΩ at the room temperature) and used to prepare all the solutions. Nitrogen (99.9%) and oxygen (99.9%) were acquired from Beijing Oxygen Factory. The polymerization and acidic solutions were de-aerated with nitrogen before the electrochemical experiments.

2.2 Apparatus

Scheme 2A (see [29] for further details) illustrates the prism-based TIRIE imaging setup used for all experiments described in this paper. A SF10 trapezoidal prism was used with an expanded light beam at 633 nm wavelength as light source and imaged with a charge coupled device (CCD) camera. The incident light beam goes through the polarizer, the compensator and the 65° prism where the evanescent wave is used as optical probe to detect structural alterations at the electrode surface. The incident light beam is reflected at the interface between the substrate and the tested solution and then passes through an analyzer and is focused on a sensing area of the CCD camera. The signal is the variation of polarized light intensity detected by the CCD camera, due to the change of polarization of the reflected light beam induced by reactions on the substrate. The image signal was recorded in 8 bit (0–256) grayscale format. As the TIRIE sensing surface, a 30 nm thick gold layer on a glass slice modified with the PAN-FeTSPP film was placed on top of the prism using index-matching oil. A custom-built electrochemical cell was then placed on top of the gold film



Scheme 2. (A) Scheme of the total internal reflection imaging ellipsometry (TIRIE) system and (B) the electrochemistry-total internal reflection imaging ellipsometry (EC-TIRIE) combination setup.

for holding the tested solution. A wound Pt wire counter electrode and a saturated calomel reference electrode (SCE) were inserted into the electrochemical cell from the top opening. A VersaSTAT 3 electrochemical system (U.S.A.) was used for controlling the working electrode potential and recording the potential and current.

Scheme 2B (see [11] for further information) shows the detailed scheme of the cell used in this work. The electrochemical cell is separated from the sample cell by an oxygen-permeable membrane. The electrolyte is then filled in the space containing the three-electrode system. DO in samples can diffuse into the supporting electrolyte through the oxygen-permeable membrane. In addition, a polydimethylsiloxane (PDMS) film is used to provide a liquid-tight seal for the electrochemical cell which established the active area of the electrode ($A \approx 0.28 \text{ cm}^2$). A commercial dissolved oxygen meter (TP 351, Beijing Timepower Measurement and Control Equipment Co, Ltd) was used to gauge oxygen concentration in samples.

PAn and PAn-FeTSPP films were also synthesized on Arrandee thin gold film electrodes, consisting of a 200 nm Au layer on borosilicate glass (with a pre-layer of 2–4 nm of chromium). Film morphology was imaged by AFM using a Nanoscope IIIa Multimode microscope (DI Veeco) in tapping mode with silicon probes and an oscillation frequency of ca. 300 kHz. The images were obtained at a scan rate of ca. 1.5 Hz.

2.3 Experimental Procedure

Prior to each experiment, the gold substrate was treated in a UV/ozone cleaner for 15 min, followed by rinsing with deionized water and high purity ethanol several times. (Caution: the UV/ozone cleaner is an extremely strong oxidant and is potentially explosive, so it should be handled with extreme caution).

PAn-FeTSPP films were grown on the gold substrate from 0.5 M H_2SO_4 containing 0.1 M aniline and 0.05 mM FeTSPP. The electro-synthesis was performed potentiodynamically for 8 cycles at a scan rate of $\nu = 20 \text{ mV s}^{-1}$. For the first five cycles the potential of the electrode was scanned from -200 to 800 mV (vs. SCE), then the anodic limit was lowered to 750 mV for the next three cycles in order to avoid over-oxidation of the PAn film [18,30].

Steady-state polarization curves of the PAn-FeTSPP film were obtained in the potential range between -200 and 400 mV vs. SCE, in 0.1 M H_2SO_4 in the presence and absence of oxygen. Potential steps of 20 mV were applied with a duration of 60 s each and the optical signal and current value were recorded at the end of this period.

After the electropolymerization, the electrochemical cell was filled with oxygen-free 0.1 M H_2SO_4 as supporting electrolyte for DO detection; a cyclic voltammogram of the modified electrode in this solution was recorded before each DO measurement. For DO assessment, an electrode potential of -200 mV (vs. SCE) was first applied for 60 s to fully discharge the film and guarantee the same initial conditions in all the experiments. Finally, DO was measured under the application of a small cathodic current ($2.5 \mu\text{A}$) to the modified electrode, by passing the sample solution (with different DO contents) through the sample cell.

2.4 Preparation of Solutions with Different Concentrations of DO

Different concentrations of DO in the sample solutions were obtained by adding sodium sulfite into air saturated 5 mM PBS solutions, in suitable amounts, taking into account the stoichiometry of the reaction $\text{SO}_3^{2-} + \frac{1}{2}\text{O}_2 \leftrightarrow \text{SO}_4^{2-}$. The DO concentrations of these samples were confirmed by the commercial dissolved oxygen meter.

3 Results and Discussion

3.1 Electrocatalytic Properties of FeTSPP toward ORR

The electrochemical activity of FeTSPP was characterized in 0.5 M H_2SO_4 solution and, in order to evaluate the catalytic activity of this iron porphyrin towards the ORR, cyclic voltammograms were recorded in the presence and absence of oxygen, and compared to control CVs registered in the absence of FeTSPP. The resulting voltammograms represented in Figure 1. In the relevant potential range and in the de-aerated solution, only one current

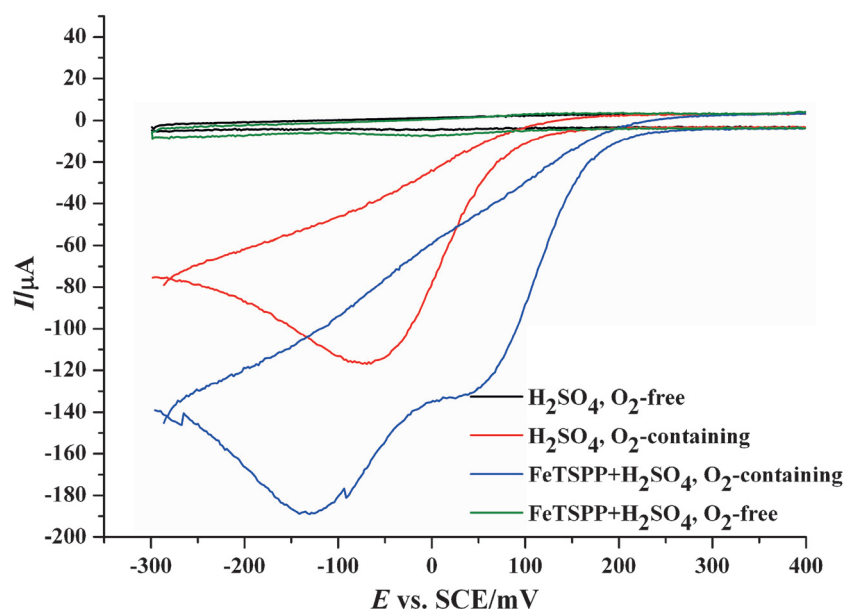


Fig. 1. Cyclic voltammograms of gold film in 0.5 M H_2SO_4 with and without 0.05 mM FeTSPP in O_2 -free and O_2 -containing solution; $\nu = 20 \text{ mV s}^{-1}$.

peak ($E \approx 0 \text{ mV}$ (vs. SCE)) can be attributed to the iron-porphyrin. This cathodic wave corresponds to the reduction of Fe(III) to Fe(II) in the FeTSPP [31].

The voltammogram obtained in the presence of oxygen reveals the catalytic activity of FeTSPP toward the ORR, as can be observed by comparing the voltammograms registered in oxygenated H_2SO_4 solution with and without the iron-porphyrin. The cathodic current generated in the FeTSPP-containing solution has an onset potential of $E \approx 200 \text{ mV}$ (representing a shift of approximately 100 mV from that recorded in the absence of FeTSPP) and a peak at $E \approx -130 \text{ mV}$ (vs. SCE) (negatively shifted by about 60 mV from that obtained without the metal-complex). The peak corresponding to the reduction of the iron within the porphyrin macrocycle is slightly shifted to a more positive potential ($E_p \approx 50 \text{ mV}$) by the presence of oxygen in solution.

The results confirm the catalytic activity of FeTSPP for the ORR. It can, therefore, be expected that the insertion of FeTSPP into the polymeric matrix of PAn will result in an increase of sensitivity of the modified electrode to oxygen due to a mediator-type effect, where the Fe(II)TSPP in the PAn matrix is oxidized by the dissolved oxygen in solution ($E_{\text{onset}} \approx 200 \text{ mV}$; $E_{\text{red}}^p \approx 100 \text{ mV}$) and subsequently regenerated (reduced) by the PAn ($E_{\text{onset}} \approx 50 \text{ mV}$; $E_{\text{ox}}^p \approx 200 \text{ mV}$ —Figure 1A Supporting Information). The extent of this process should be dependent on the quantity of DO that the PAn-FeTSPP film is exposed to, and it should be reflected in the color and refractive index of the film, as well as in the measured potential of the system.

3.2 Electrochemical Synthesis of PAn-FeTSPP

Figure 2 shows the cyclic voltammograms recorded during the polymerization of aniline in the presence of FeTSPP and the simultaneously registered TIRIE optical response of the electrode surface. In the first potential scan it can be noted (Figure 2A) that the current increases at potentials higher than 750 mV (vs. SCE), corresponding to the monomer oxidation and formation of the first nuclei of the polymer. It is worth of notice that this feeble modification of the surface can be perceived by the TIRIE optical monitoring of the electrode (Figure 2B). In the backward potential scan, a cathodic wave with an onset potential of $E \approx 200 \text{ mV}$ (vs. SCE) and centered at $E \approx -100 \text{ mV}$ (vs. SCE) must be attributed to the presence of FeTSPP in solution since it did not occur during the polymerization of aniline on gold in the absence of the metal-complex [11,32]. The thickening of the film upon repetitive potential cycling is evidenced by the continuous increase of the height of the polymer redox peaks in the potential range -100 to 300 mV (vs. SCE). The magnitude of the optical changes displayed in Figure 2B increases accordingly with the polymer thickening, and reveals significant differences from the oxidized to the reduced state of the film. Those signal modifications result from the well-known chromatic conversions of the PAn corresponding to its actual redox state. The electrochemical response of the FeTSPP is masked by that of the PAn, as evidenced by the displacement of the reduction peak potential for the typical values of the PAn films. Nevertheless, the higher reduction charge (recorded in the potential interval where the redox conversion of the film takes place) compared to the oxidation charge, indicates that the anionic organometallic complex that is

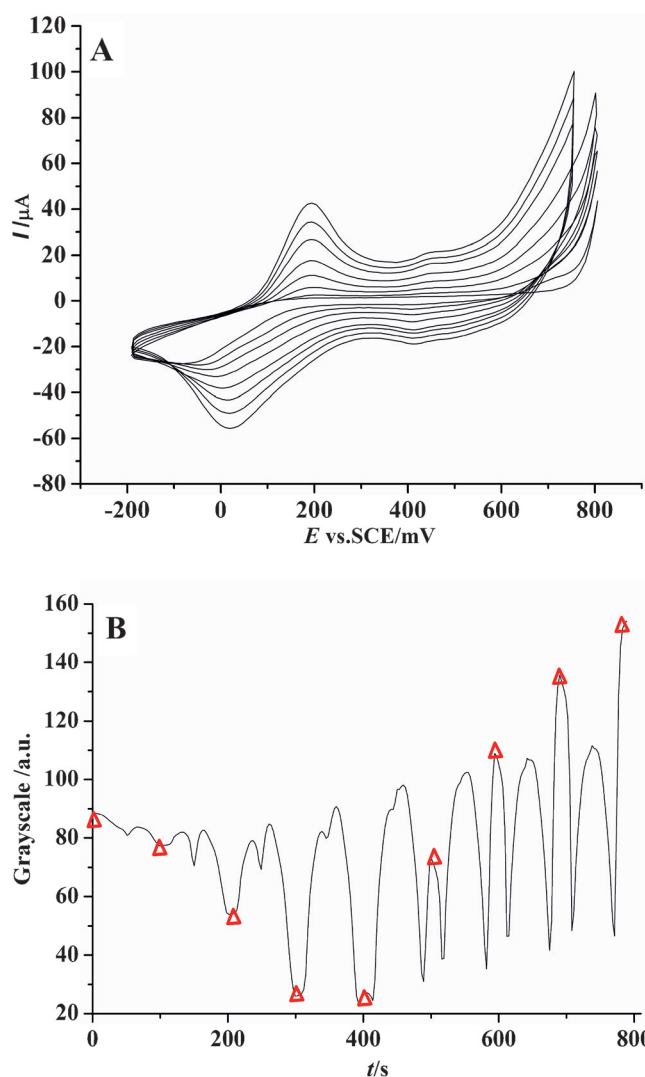


Fig. 2. Electrolysis of PAn-FeTSPP; aniline 0.1 M, FeTSPP 0.05 mM, H_2SO_4 0.5 M; $\nu = 20 \text{ mV s}^{-1}$: (A) cyclic voltammograms, (B) TIRIE optical response. The red triangles in (B) correspond to the values of grayscale registered at the cathodic potential limit (-200 mV).

being incorporated as counter ion in the anodic scan, is not completely expelled during the polymer reduction, and part of it remains entrapped in the polymer matrix.

Figure 2B shows clearly (see red triangles) that the optical properties of the film change significantly from cycle to cycle, namely in the negative potential range. Further experiments (not shown) demonstrate that the magnitude of the variation of the optical signal upon redox conversion of the film did not increase significantly for films synthesized with more than 8 growth cycles in our conditions. On the other hand, for TIRIE measurements, it is important to keep the film thickness as thin as possible since the thickness of the film must be within the probe depth of the evanescent wave (about 100 nm). It was therefore decided to prepare the PAn-FeTSPP films for DO monitoring with only eight growth cycles.

3.3 Morphological Characterization of PAn-FeTSPP

Figure 3 depicts AFM images of PAn and PAn-FeTSPP films grown on thin layer Au surfaces under the same electrochemical conditions. Figure 3A shows that the electrode surface is completely covered by PAn, and that the polymer has a globular morphology that is typical for such materials [33]. In Fig. 3B it can be seen that, the presence of FeTSPP has a drastic effect on the morphology of the film, exhibiting cylindrical shaped filaments covered by polymer growing outwards. The explanation for this behaviour is the well-known formation of porphyrin J aggregates in acidic aqueous solutions [34], which originates such tri-dimensional arrangement. A six-fold increase in the root mean square roughness (R_q) from 2 nm with the PAn films to 12 nm, in the presence of the por-

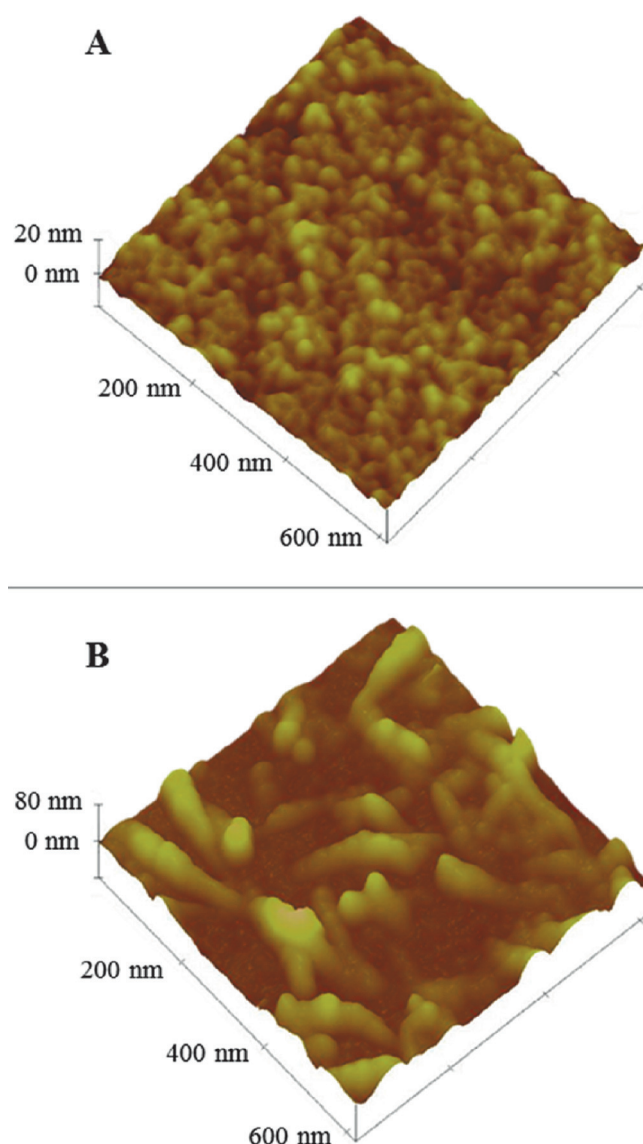


Fig. 3. Morphology images of (A) PAn and (B) PAn-FeTSPP films synthesized under the same conditions as described in Figure 2.

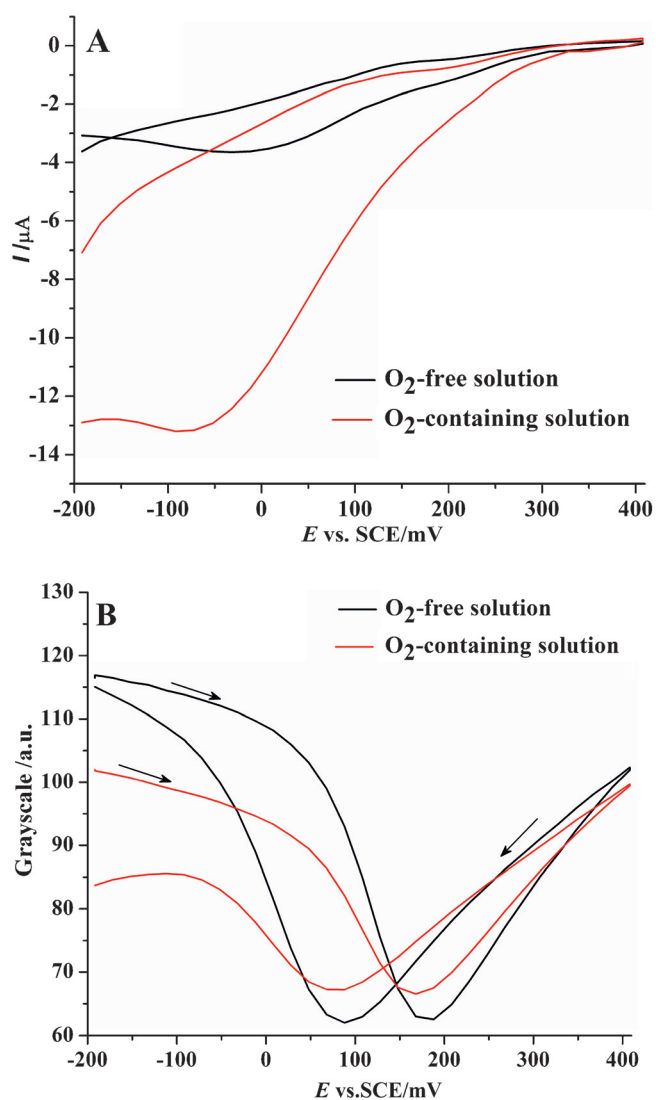


Fig. 4. (A) Steady state polarization curve and (B) simultaneous TIRIE characterization of the PAn-FeTSPP film in 0.1 M H₂SO₄. The O₂-containing solution has a DO concentration of ca. 12.8 mg L⁻¹.

phyrin moiety is observed. The topography of the modified electrode strongly suggests that the interaction of the oxygen with the catalyst should be mainly a surface phenomenon due to the high exposed active area.

3.4 Electrochemical and Optical Response of PAn-FeTSPP to DO

Steady state polarization curves of the electrode modified by PAn-FeTSPP were registered and accompanied by TIRIE in O₂-free and O₂-containing H₂SO₄ (0.1 M) solution.

These results, represented in Figure 4, confirm the affinity of the PAn-FeTSPP towards oxygen. In the presence of oxygen, the modified electrode exhibits a high catalytic activity for the dioxygen reduction with an onset potential of about 0.3 V vs. SCE. Due to the steady-state

conditions imposed to the system, the redox conversion of the polymer is not evident in these experiments (see Figure 3 Supporting Information for the curves recorded at $v = 20 \text{ mV s}^{-1}$). Nevertheless, the processes corresponding to the leucoemeraldine – emeraldine transition (both the reduction and oxidation of the PAn matrix) were detected by TIRIE – Figure 4B.

This sensitivity to oxygen is a consequence of the incorporated FeTSPP in the PAn matrix, since it is not observed with the PAn polymer (see Figure 1 Supporting Information). The optical data obtained during this characterization gives us important information about the maximum range of grayscale values which can be obtained with the modified electrode and indicates the optimal potential range for DO detection. Figure 4B shows a hysteresis between the anodic (forward) and cathodic (backward) scans, which can be attributed to the structural and morphologic modifications that all conducting polymers suffer during their redox processes [32,35,36]; Since the redox conversion of any polymer film involves mechanical deformation of the matrix (with simultaneous intake and/or expulsion of solvent and counter-ions), high activation overpotentials are required both for oxidation as well as for reduction, resulting in a significant redox hysteresis. In the absence of oxygen the grayscale values are at a maximum when the modified electrode is in its reduced state. As the potential increases, the grayscale values decrease with a slow slope at first, steeply as the polymeric matrix is oxidized. After reaching a minimum at $E \approx 200 \text{ mV}$ (corresponding to the transition leucoemeraldine – emeraldine), the grayscale values rise slowly, reaching a local maximum at the anodic potential limit of the polarization curve as the polymer is being further oxidised. In the cathodic sweep, the graph has a similar shape, with a slight shift to more negative potentials. In the oxygenated solution the overall optical features are similar with the exception of behaviour at the more negative potential region where the grayscale value corresponds to a partially oxidised state of the film caused by the presence of the oxygen.

Based on the data obtained during the electrochemical and optical characterization, it is evident that the ideal potential range for the DO detection is where the steepest change in grayscale as a function of the applied potential occurs, i.e. between the maximum ($E \approx 0 \text{ mV}$) and minimum ($E \approx 200 \text{ mV}$) of grayscale registered during the anodic scan. The grayscale values registered during the coupled electrochemical/optical experiments confirm that there is significant change in the optical properties of the film during its doping/dedoping process.

The modified electrode was initially extensively discharged to the neutral state by submitting the film to a potential of -0.2 V for 60 s (time large enough to the current fall to negligible values). After this procedure the electric and optical response of the surface was monitored under open circuit conditions and a stabilization of the grayscale values was achieved for $t \geq 400 \text{ s}$ with a difference of only ≈ 4.7 units in the presence and absence of

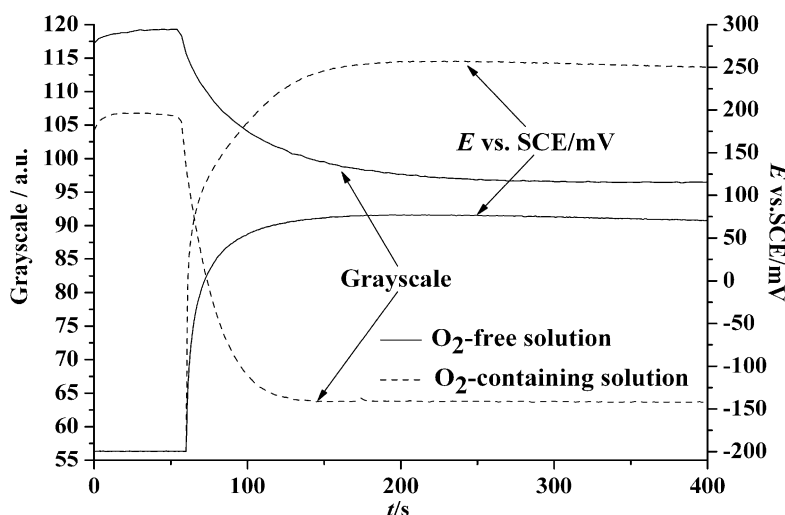


Fig. 5. Real time potential and grayscale curves of PAN-FeTSPP to DO; Conditions: 0.1 M H₂SO₄; initially, $E = -200$ mV was applied for 60 s followed by the application of a cathodic current of $I_{\text{appl}} = -2.5$ μA . The O₂-containing solution has a DO concentration of ca. 16.5 mgL⁻¹.

dissolved oxygen (see Figure 2 Supporting Information). The corresponding open circuit potentials of the PAN-FeTSPP modified electrode were about 250 mV and 330 mV in O₂-free and O₂-containing sulfuric acid solutions, respectively. Actually, for potential values higher than 0.2 V, the grayscale values changes only slightly with the electrode potential. In order to negatively shift the potential values to a more favourable region (higher variation of the optical signal with the electrode potential) and simultaneously increase the difference of the potential (and, consequently, in the chromism) exhibited by the modified electrode in the presence and absence of oxygen, a small cathodic current was applied to the electrode after the polymer discharge.

This galvanostatic condition results in a shift of the electrode potential to the typical values corresponding to the oxygen reduction (according with its concentration) in such polymer, while in the absence of oxygen the electrode potential will be driven to much lower potential values in order to maintain the imposed cathodic current. The magnitude of the applied current was carefully optimized to tune the potential values into the region where the grayscale changes are greatest. Figure 5 shows the evolution of the electrical potential of the PAN-FeTSPP-modified Au electrode during the application of a cathodic current ($I_{\text{appl}} = -2.5$ μA) in O₂-free and O₂-containing 0.1 M H₂SO₄ solution, following the initial discharge period ($E = -200$ mV (vs. SCE); $t = 60$ s). The data show that both electrochemical (potential) and optical parameters stabilize at $t \approx 180$ s, i.e. after applying I_{appl} for 120 s. The measured potential for $t \geq 180$ s is 75 mV in the absence of oxygen, 250 mV in its presence ($\Delta E \approx 175$ mV). The difference between the values in grayscale registered for the O₂-free and O₂-containing solution is, approximately, 33 grayscale units.

To evaluate the suitability of the PAN-FeTSPP modified electrode to be employed in a DO sensor, its re-

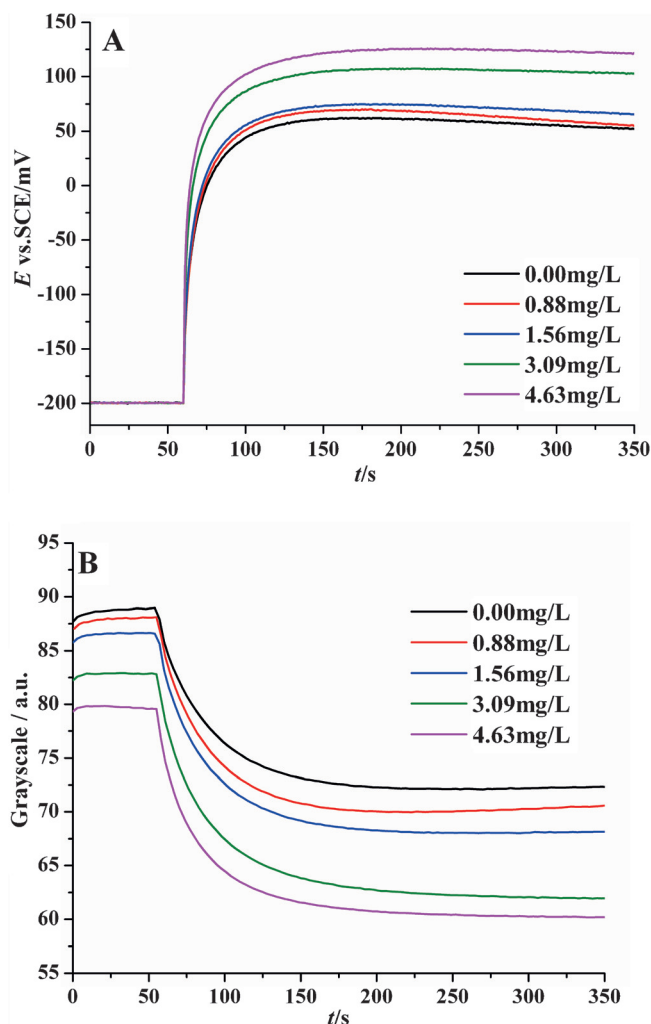


Fig. 6. (A) Electrode potential and (B) grayscale variation with time of the PAN-FeTSPP-modified electrode exposed to different concentrations of DO; Conditions: 0.1 M H₂SO₄; initially, $E = -200$ mV was applied for 60 s followed by the application of a cathodic current of $I_{\text{appl}} = -2.5$ μA .

Table 1. Comparison of the sensitivity of the combination sensor with previously reported works. β CDSAuNP: β -cyclodextrin-modified gold nanoparticles; FeT4MPyP: iron(III) tetra(*N*-methyl-4-pyridyl)-porphyrin; CoTSPc: cobalt tetrasulfonated phthalocyanine; PLL: poly-L-lysine; PFeTMHPP: polymerized iron(III) tetra(3-methoxy-4-hydroxy-phenyl) porphyrin; PEDOT: poly(3,4-ethylenedioxythiophene); GC: glassy carbon; DPV: differential pulse voltammetry.

S. N.	Modified electrode	Technique	DO range (mg L ⁻¹)	Sensitivity	Ref
1	Nickel- <i>salen</i> polymer film/Pt	Amperometry	3.95–9.2	13.77 $\mu\text{A mg}^{-1} \text{L cm}^{-2}$	[4]
2	β CDSAuNP/ FeT4 MPyP/Au	Amperometry	0.2–6.5	25.5 $\mu\text{A mg}^{-1} \text{L cm}^{-2}$	[37]
3	CoTSPc/PLL/GC	Amperometry DPV	0.2–8.0	11 $\mu\text{A mg}^{-1} \text{L cm}^{-2}$ 18.3 $\mu\text{A mg}^{-1} \text{L cm}^{-2}$	[38]
4	Pt/C/Nafion composite	Amperometry	1.24–5.15	1.74 $\mu\text{A mg}^{-1} \text{L cm}^{-2}$	[39]
5	SiO ₂ /SnO ₂ /MnPc disk	Amperometry	0–8.1	4.59 $\mu\text{A mg}^{-1} \text{L cm}^{-2}$	[40]
6	PFeTMHPP/Pt	Amperometry	0–10	25.43 $\text{nA mg}^{-1} \text{L cm}^{-2}$	[41]
7	PEDOT/iron oxalate film/Pt	Amperometry	0–20	9.91 $\mu\text{A mg}^{-1} \text{L cm}^{-2}$	[42]
8	Cu _{0.4} Ru _{3.4} O ₇ + RuO ₂ /Al ₂ O ₃	Potentiometric	0.8–8	46 mV per decade	[43]
9	PAn/Au	Potentiometric	0.85–16.57	15 mV per decade 2.62 G per decade	[11]
10	PAn-FeTSPP film/Au	Potentiometric TIRIE	0–4.63	13.39 mV mg ⁻¹ L 4.18 G mg ⁻¹ L	This work

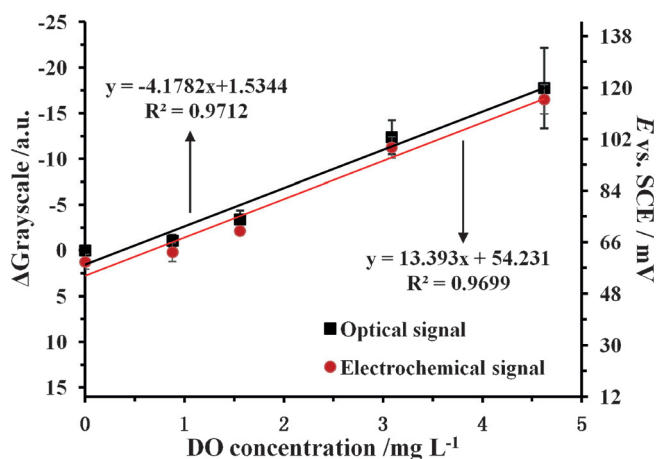


Fig. 7. Electrode potential and grayscale recorded at $t=300$ s of the PAN-FeTSPP-modified electrode exposed to different concentrations of DO; Conditions: 0.1 M H₂SO₄; initially, $E=200$ mV was applied for 60 s followed by the application of a cathodic current of $I_{\text{appl}} = -2.5 \mu\text{A}$.

response to samples with different concentrations of DO was monitored by the coupled EC-TIRIE system. The electrochemical and optical response of the modified surface to different contents of oxygen in the test solutions are displayed in Figure 6, and represented against the oxygen content of the sample solution in Figure 7 (data collected at $t=300$ s). The results confirm the ability of such a modified electrode to monitor the DO content of aqueous solutions using the combined EC-TIRIE sensor. Both electrochemical and optical signals are significantly increased when compared with those obtained with bare gold or PAn [11], revealing a high sensitivity to very low amounts of DO. Furthermore, the galvanostatic control of the electrode rendered the detection method much faster than when undertaken under equilibrium conditions.

Table 1 compares the sensitivities and DO ranges of applicability of different sensors reported in the literature. Most DO sensors are amperometric, so a direct compari-

son of these sensitivities with that of the system studied in this work is not possible. Nevertheless, among those with potentiometric transduction, the response of the PAN-FeTSPP modified electrode for low DO concentrations is, by far, much better than the other reported probes. Furthermore, the potentiometric approach is less sensitive to variations of the conductivity (ionic strength) of the sample solutions than the amperometric method.

4 Conclusions

Polyaniline films containing entrapped Fe(III) meso-tetra(4-sulfonatophenyl) porphyrin (FeTSPP) anions (PAN-FeTSPP) have been prepared and revealed high sensitivity towards the presence of DO, keeping the typical electrochemical reversibility of PAn. Employed in an EC-TIRIE sensor, the PAN-FeTSPP-modified Au electrode revealed much higher sensitivity to DO than a thin gold film or PAn-modified gold electrode, even for very low oxygen concentrations. The galvanostatic control by the application of a small cathodic current to the electrode also reduces significantly the response time of the sensor and tunes the redox state of the modified electrode to the more responsive region of the polymeric probe. The combined electrochemical and optical signals strongly corroborate each other, allowing the normalization of the readings in repetitive measurements using the same modified electrode.

Acknowledgements

Authors acknowledge the financial support to the *National Basic Research Program of China (2009CB320302)*, the *National High Technology Research Development Program of China (2008AA02Z419)*, the *International Science & Technology Cooperation Program of China (2012DFG31880)* and *Projects of Sino-Portugal S&T Cooperation 2010–2015, Fundação para a Ciência e a Tecnologia (project PTDC/QUI-QUI/121857/2010)*, the *National*

Natural Science Foundation of China (21305147), and the Instrument Developing Project of the Chinese Academy of Sciences (KJCX2-YW-M04, KJCX2-YW-M03).

References

- [1] C.-S. Chua, Y.-L. Lo, *Sens. Actuators B* **2010**, *151*, 83.
[2] X. B. Na, W. C. Niu, H. W. Li, J. X. Xie, *Sens. Actuators B* **2002**, *87*, 222.
[3] S. Zhuiykov, E. Kats, *Sens. Actuators B* **2013**, *187*, 12.
[4] C. S. Martin, T. R. L. Damos, M. F. S. Teixeira, *Sens. Actuators B* **2012**, *175*, 111.
[5] S. Zhuiykov, K. Kalantar-zadeh, *Electrochim. Acta* **2012**, *73*, 105.
[6] S. K. Lee, I. Okura, *Spectrochim. Acta A* **1998**, *54*, 91.
[7] C. Pulido, Ó. Esteban, *Sens. Actuators B* **2013**, *184*, 64.
[8] C.-S. Chu, Y.-L. Lo, *Sens. Actuators B* **2011**, *155*, 53.
[9] L. Nei, R. G. Compton, *Sens. Actuators B* **1996**, *30*, 83.
[10] R. G. Compton, R. J. Northing, *J. Chem. Soc. Faraday Trans.* **1990**, *86*, 1077.
[11] M. Li, W. Liu, J. P. Correia, A. C. Mourato, A. S. Viana, G. Jin, *Electroanalysis* **2014**, *26*, 374.
[12] R. S. Saberi, S. Shahrokhian, G. Marrazza, *Electroanalysis* **2013**, *25*, 1373.
[13] G. Inzelt, *Conducting Polymers: a New Era in Electrochemistry*, Springer, New York, **2008**, pp. 16.
[14] Y. B. Shim, D. E. Stilwell, S. M. Park, *Electroanalysis* **1991**, *3*, 31.
[15] A. M. Wu, E. C. Venancio, A. G. MacDiarmid, *Synth. Met.* **2007**, *157*, 303.
[16] Y. F. Li, R. Y. Qian, *Synth. Met.* **1993**, *53*, 149.
[17] D. K. Moon, M. Ezuka, T. Maruyama, K. Osakada, T. Yamamoto, *Macromolecules* **1993**, *26*, 364.
[18] D. E. Stilwell, S. M. Park, *J. Electrochem. Soc.* **1988**, *135*, 2254.
[19] V. G. Khomenkol, V. Z. Barsukov, A. S. Katashinskii, *Electrochim. Acta* **2005**, *50*, 1675.
[20] E. K. W. Lai, P. D. Beattie, S. Holdcroft, *Synth. Met.* **1997**, *84*, 87.
[21] M. J. Croissant, T. Napporn, J. M. Leger, C. Lamy, *Electrochim. Acta* **1998**, *43*, 2447.
[22] T. Sawaguchi, T. Matsue, K. Itaya, I. Uchida, *Electrochim. Acta* **1991**, *36*, 703.
[23] A. Okunola, B. Kowalewska, M. Bron, P. J. Kulesza, W. Schuhmann, *Electrochim. Acta* **2009**, *54*, 1954.
[24] L. Birry, J. H. Zagal, J. P. Dodelet, *Electrochem. Commun.* **2010**, *12*, 628.
[25] T. S. Olson, K. Chapman, P. Atanassov, *J. Power Sources* **2008**, *183*, 557.
[26] K. Yamamoto, D. Taneichi, *J. Inorg. Organomet. Polym. Mater.* **1999**, *9*, 231.
[27] X. Y. Xie, Z. F. Ma, X. X. Ma, Q. Z. Ren, V. M. Schmidt, L. Huang, *J. Electrochem. Soc.* **2007**, *154*, B733.
[28] P. A. Forshey, T. Kuwana, *Inorg. Chem.* **1981**, *20*, 693.
[29] L. Liu, A. Viollat, G. Jin, *Sens. Actuators B* **2014**, *190*, 221.
[30] M. T. S. Chani, K. S. Karimou, F. A. Khalid, S. A. Moiz, *Solid State Sci.* **2013**, *18*, 78.
[31] A. J. Bard, M. Stratmann, G. S. Wilson (Eds.), *Encyclopedia of Electrochemistry, 1st edition., Vol. 9*, John Wiley & Sons, Inc, New York, **2002**, pp. 196.
[32] L. M. Abrantes, J. P. Correia, G. Jin, *Electrochim. Acta* **2001**, *46*, 3993.
[33] A. Mourato, A. S. Viana, J. P. Correia, H. Siegenthaler, L. M. Abrantes, *Electrochim. Acta* **2004**, *49*, 2249.
[34] S. M. Andrade, P. Raja, V. K. Saini, A. S. Viana, P. Serp, S. M. B. Costa, *ChemPhysChem* **2012**, *13*, 3622.
[35] L. M. Abrantes, J. P. Correia, M. Savic, G. Jin, *Electrochim. Acta* **2001**, *46*, 3181.
[36] L. M. Abrantes, J. P. Correia, A. I. Melato, *J. Electroanal. Chem.* **2010**, *646*, 75.
[37] F. S. Damos, R. C. S. Luz, A. A. Tanaka, L. T. Kubot, *Anal. Chim. Acta.* **2010**, *664*, 144.
[38] R. C. S. Luz, F. S. Damos, A. A. Tanaka, L. T. Kubot, *Sens. Actuators B* **2006**, *114*, 1019.
[39] Y. C. Liu, B. J. Hwang, I. J. Tzeng, *Electroanalysis* **2001**, *13*, 1441.
[40] L. S. S. Santos, R. Landers, Y. Gushikem, *Talanta* **2011**, *85*, 1213.
[41] X. Z. Wu, Y. J. Li, B. Grundig, N. T. Yu, R. Renneberg, *Electroanalysis* **1997**, *9*, 1288.
[42] G. Bencsik, Z. Lukács, C. Visy, *Analyst*, **2010**, *135*, 375.
[43] S. Zhuiykov, K. Kalantar-zadeh, *Electrochim. Acta* **2012**, *73*, 105.

Received: November 16, 2014

Accepted: December 27, 2014

Published online: March 5, 2015